

# OPTIMIZATION OF HORIZONTAL AXIS WIND TURBINE DESIGN AND PERFORMANCE IN ARRAY ARRANGEMENT FOR MALAYSIAN SEAS

Farah Ellyza Binti Hashim<sup>a</sup>, Jie Heng Goh<sup>a</sup>, Wei Han Khor<sup>a</sup>, Chee Loon Siow<sup>b\*</sup>

<sup>a</sup>Department of Aeronautics, Automotive and Naval Architecture, Faculty of Mechanical Engineering, Universiti Teknologi Malaysia

<sup>b</sup>Marine Technology Center, Universiti teknologi Malaysia

## Article history

Received

7<sup>th</sup> August 2025

Received in revised form

7<sup>th</sup> November 2025

Accepted

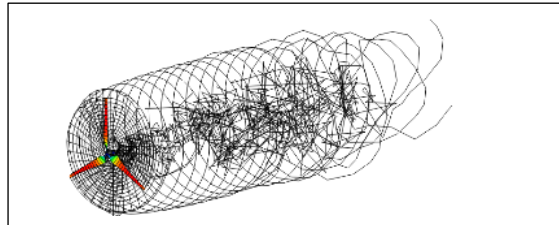
7<sup>th</sup> November 2025

Published

10<sup>th</sup> December 2025

\*Corresponding author  
scheeloon@utm.my

## GRAPHICAL ABSTRACT



identifies an optimal 150 m rotor with 6° attack achieving  $C_p = 0.5$ , demonstrating that design re-tuning for low-speed monsoonal winds can yield 20 MW-class power outputs from compact staggered arrays.

## ABSTRACT

Malaysia offshore regions have the potential for the development of the Horizontal Axis Wind Turbine (HAWT) wind turbine, where the annual mean wind speed is greater than 4 m/s. Although the annual wind speed meets the minimum requirement for wind turbines to generate electricity, the steady wind flow is still lower compared to other countries. Therefore, the purpose of this paper is to optimize the parameters of the wind turbine blades to improve the performance and power production of HAWT for the usage in Malaysian sea. The performance and power production of optimized turbines in array arrangement is also investigated. Computational analysis using software Qblade was performed to evaluate the result of power production of blade properties including blade diameter and blade angle of attack, while Computation Fluid Dynamic (CFD) is used to evaluate the performance in array arrangement when subjected to Malaysia sea conditions. This study advances prior offshore wind optimization work by addressing the underexplored tropical low-wind regime of Malaysia. The integrated Qblade–CFD approach

## KEYWORDS

Computational analysis; Horizontal Axis Wind Turbine; Low Wind Speed; Renewable Energy, Wind Farm.

## INTRODUCTION

According to the Global Wind Report 2021 proposed by Global Wind Energy Council (GWEC), a total of 743 GW of wind power capacity has been installed worldwide today and helping to avoid over 1.1 billion tonnes of CO<sub>2</sub> globally [1]. Among the countries who developed the wind energy, China is the world leader in wind energy development, with over one-quarter of the world's power capacity of 342 GW wind capacity installed. The windfarm built in China normally is onshore where the world's largest onshore windfarm built out of the Gobi Desert in Gansu Province with 10 GW peak capacity generated along the way. Next, the largest wind energy developer is the United States, which had a cumulative installed wind capacity of 139 GW in 2021. The world's second largest windfarm is located at the Alta Wind Energy Centre in California with a capacity of 1.548 GW. However, current wind energy

installations are insufficient to achieve net zero CO<sub>2</sub> emissions by 2050. The world must install wind energy three times faster in the coming decades to meet this target and mitigate climate change impacts.

Renewable energy provides a clean and eco-friendly energy source. It is more established in developed countries as the operation cost is cheaper and cleaner than fossil fuels. The implementation of renewable energy is not that significant in Malaysia yet due to the huge dependency on fossil fuel as the main source of energy. Located at the equatorial, Malaysia's sea conditions vary throughout the year, with monsoon seasons affecting the coastal waters, causing strong winds, choppy waves, and heavy rainfall. The South China Sea is considered a potential location for developing wind farms taking into account the relatively shallow sea and wind speeds due to consistent monsoon winds. The relatively shallow sea depth makes it suitable for offshore wind farms as they can be erected on the continental shelf, whereas the monsoon winds provide relatively high wind speeds [2].

Malaysia's exclusive economic zone (EEZ) in the South China Sea experiences annual wind speeds exceeding 4 m/s [3]. Within this zone, three promising locations in Terengganu, Sarawak, and Sabah have been identified, each boasting an average wind energy potential of over 300 kWh/m<sup>2</sup>/year. For example, a study conducted by Albani et al. (2013) [2] evaluated the feasibility of exploiting wind energy in Kijal, Terengganu. The turbine capacity of 850kW was able to generate an annual energy production (AEP) of 26.8 million kWh per year. The results also show an 8-year payback period for offshore wind projects and a proposed Feed in Tariff (FiT) rate of 0.81 to 1.38 MYR.

Wind energy is a clean and sustainable resource with the potential to become the principal source of electric energy on a global scale in the future. Nevertheless, the potential of wind energy varies significantly depending on the geographic conditions of each nation. The capability of wind turbines to efficiently convert local wind into electric energy is critical for determining the suitability of wind turbine installations. Given the varying wind potential, it is essential to optimise the parameters of the wind turbine to meet specific operational requirements. Premono et al. (2016) [4] investigated wind speed and the potential for wind energy in the northern coastal region of Semarang, Indonesia. The annual mean wind

speed for the selected locations was recorded at 5.32 m/s, with a maximum annual energy velocity of 6.45 m/s. The necessary cut-in speed of the wind turbine ranged from 2.7 m/s to 4.5 m/s among turbines from different manufacturers, illustrating the discrepancy in performance among turbines with varying aerodynamic profiles. Yass et al. (2018) [5] explored the optimisation of wind turbine blades regarding different blade cross sections. The analysis utilised various coding techniques to optimise the blade chord and lift-to-drag ratios in relation to the blade pitch angle. This optimisation of blade chord and lift-to-drag twist resulted in a power coefficient increase of 10.3% and 9.5% for Eppler 4417 and NACA 4412, respectively.

The performance of wind turbine in wind farm arrays are also essential to further ensure the possibility of wind farm installation in Malaysia. The design process of wind farm layout is advantageous for maximizing energy production, minimizing capital and operating costs, and staying within the constraints imposed by the site. Consider the design of wind farm arrangement, separation distances between turbines, distance from shore, and wind direction. Turbine arrangement leads to a higher velocity deficit from the wake [6]. Adequate separation between the wind turbines in a wind farm must be obtained to minimize the energy loss due to wind shadowing from upstream turbines [7].

Shin et al. (2021) [8] examined the best configuration of wind turbines to enhance energy production by minimising energy losses caused by wakes in a constrained area. A metamodeling method was used to replace expensive simulation and physical experiments. They studied patterns of turbine layout, such as coastline distance, base angle, side angle and column angle, and identified that the column distance arrangement of wind turbines produced the highest AEP of 169 GWh per year with 8.5% wake loss and 26.1% capacity factor. This shows the significance of considering arrangement pattern when designing a wind far, as the arrangement pattern highly contributes to the increase in power generating efficiency.

Although the annual wind speed in Malaysia is seasonal, it still meets the minimum requirement for wind turbines to generate electricity. To exploit low wind energy, optimize the wind turbine for Malaysia's wind characteristics and select an appropriate wind farm layout to enhance power generation

efficiency. Therefore, the purpose of this paper aims to optimize the parameters of the wind turbine blades to improve the performance and power production of HAWT for the usage in Malaysian sea. The performance and power production of optimized turbines in array arrangement is also investigated. Computational simulation to optimize the wind turbine blades is conducted using Qblade, whereas the selection of wind farm arrangement is attained using CFD. To suit the geographical scope of Malaysia's EEZ, the location is limited to the southern part of South China sea with an annual average speed of 2 to 6 m/s [3]. The potential location for selecting the arrangement for wind farm is Kijal, Terengganu [2]. The incident wind speed used to determine the performance of wind turbines in array arrangement is maintained at a steady flow of 5.364 m/s.

While many optimization studies have focused on HAWT performance under moderate to high wind regimes typical of temperate offshore sites, fewer efforts have examined design adaptation for low-wind tropical seas, where wind speeds often range from 3–6 m/s. This study contributes by integrating aerodynamic optimisation using Qblade with CFD-based array performance analysis tailored to Malaysia's monsoonal wind characteristics. In doing so, it establishes a methodological framework for optimizing turbine design and layout specifically for tropical offshore environments, bridging the knowledge gap between conventional offshore optimization and emerging Southeast Asian low-wind applications.

## THEORETICAL BACKGROUND

In regard to the performance of a wind turbine, the lift and drag coefficient are important parameters that should be determined. The form of the lift coefficient ( $C_L$ ) and drag coefficient ( $C_D$ ) can be written as follow:

$$C_L = \frac{L}{0.5\rho Av^2} \quad \text{Eq. 1}$$

$$C_D = \frac{D}{0.5\rho Av^2} \quad \text{Eq. 2}$$

where  $\rho$  is the density of air,  $A$  is an effective project area and  $v$  is wind speed.

The Power Coefficient ( $C_P$ ) is defined as the ratio of the actual power ( $P_T$ ) to the total power

of the wind, which flows through the wind blades at particular wind speed ( $P_O$ ). The power coefficient is affected by the operation condition which includes the wind speed, blade angle of attack and so forth. The Power Coefficient ( $C_P$ ) can be written as follow:

$$C_P = \frac{P_T}{P_O} = \frac{\frac{1}{4}\rho A(V_1^2 - V_2^2)(V_1 + V_2)}{\frac{1}{2}\rho V_1^3 A} \quad \text{Eq. 3}$$

where  $V_1$  and  $V_2$  is the wind speed at upstream and downstream of the wind turbine blades respectively. The Power Coefficient ( $C_P$ ) can also be written as a function of axial induction factor (a) as follow:

$$C_P = 4a(1 - a)^2 \quad \text{Eq. 4}$$

where axial induction factor (a) is the fractional decrement in the wind speed between the upstream and the wind turbine rotor. Next, the Thrust Coefficient ( $C_T$ ) as a function of the axial induction factor can be written as follow.

$$C_T = 4a(1 - a) \quad \text{Eq. 5}$$

The actual power produced by the wind turbine will be based on the following formula.

$$P_T = \frac{1}{2}\rho \cdot \text{TSA} \cdot V^3 \cdot C_P \quad \text{Eq. 6}$$

Where  $\rho$  is the density value of air, TSA is the turbine swept area ( $m^2$ ) and  $V$  is the wind velocity.

## METHODOLOGY

The optimization all wind turbine blade design is conducted using Qblade to evaluate the effect of blade properties, such as blade diameter and blade angle of attack on the power production, whereas ANSYS Fluent is used to estimate the performance of the wind turbine in array arrangement.

Given the low wind speeds of 2 to 6 m/s, the NACA series is chosen for its superior performance in such conditions, owing to its high lift-to-drag coefficients. In accordance to Hong et al. (2019) [9], the NACA series, especially NACA4412 has higher lift to drag ratio of 110.2929 at the angle attack of 6 degrees, which proves the superiority of NACA in terms of

aerodynamic performance. Figure 1 illustrates the profile of NACA 4412 Airfoil.

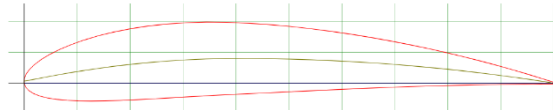


Figure 1: Profile of NACA 4412 Airfoil

For simulation of NACA 4412 in Qblade simulation, the Reynolds number used is 1000000. The chord length,  $C$  can be calculated using Eqn. 7 and 8, where  $B$  is the number of blades,  $\lambda$  is the tip speed ratio and  $D$  is the rotor diameter. The number of blades used is 3, while the tip speed ratio,  $\lambda$  is 6. The range of turbine diameter is from 20m to 170m. The chord length is calculated accordingly and shown in Table 1. Figure 2 shows the blade modeling of wind turbine blade diameter of 10m. Optimization of 6 tip speed ratio is conducted for all the blade diameters. Then, the power production is estimated the performance of the wind turbine with variation of wind speed within the range of 2m/s to 6m/s

$$\lambda = \sqrt{\frac{80}{B}} \quad \text{Eq. 7}$$

$$C = \frac{4D}{\lambda^2 B} \quad \text{Eq. 8}$$

Following the turbine blade optimisation, the wind turbine's performance in wind farm arrays is assessed using CFD. The performance of wind turbines is examined in side-by-side, triangular, and staggered arrangements. Figure 4 shows the wind turbines in triangular arrangement inside CFD interface. The distance between wind turbines for the perpendicular flow direction is selected to range from 3D to 7D based on Choi et. al [10], while the parallel separation distance between wind turbines is ranging from 3D to 5D. A distance between two groups of wind turbines should be at least 25D according to Wu et.al [11] to reduce the wake generation in the downstream wind. However, due to the computational limitation in this study, a group distance of 3D to 10D is selected to be tested on the wind farm's performance.

The test matrix to study the influence of parallel, perpendicular and group separation distance between wind turbines is as tabulated in Table 2. Case 1 to 3 is 3 turbines in side-by-side arrangement, while Case 4 to 18 is 3

turbines in triangle arrangement. Case 19 to 26 is 6-turbines staggered arrangement, where the optimum parallel and perpendicular separation is then used in the staggered layout to study the group separation distance.

Table 1: Chord length for different rotor diameter

Diameter (m)	Chord length (m)
20	1.0
30	1.5
40	2.0
50	2.6
60	3.0
70	3.6
80	4.0
90	4.6
100	5.0
110	5.6
120	6.0
130	6.7
140	7.2
150	7.7
160	8.5
170	9.0

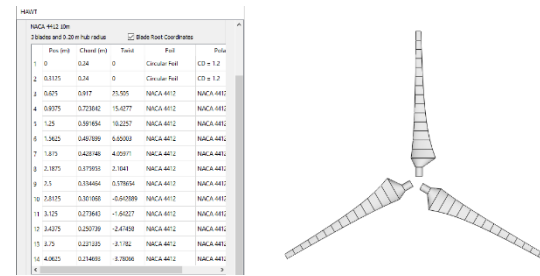


Figure 2: Design of a Horizontal Axis Wind Turbine with a Diameter of 10m and Three Blades.

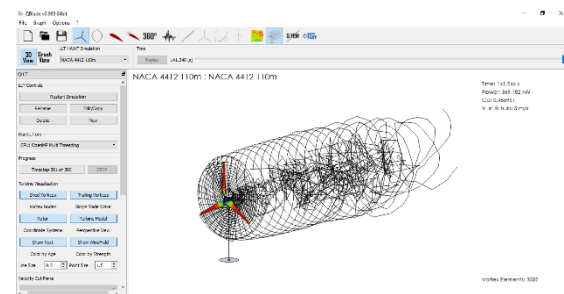
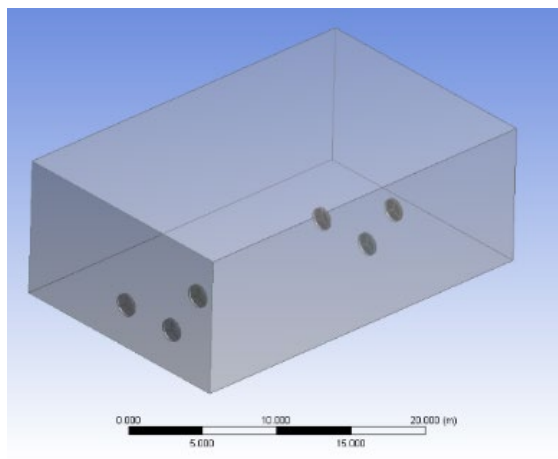


Figure 3: Three-blade horizontal axis wind turbine simulation in Qblade



**Figure 4:** Triangular wind turbine arrangement.

**Table 2:** Test Matrices of The Study

Case	Arrangement	Perpendicular Distance	Parallel Distance	Group Distance
1	Side-by-Side	N.A.	3D	N.A.
2	Side-by-Side	N.A.	4D	N.A.
3	Side-by-Side	N.A.	5D	N.A.
4	Triangular	3D	3D	N.A.
5	Triangular	4D	3D	N.A.
6	Triangular	5D	3D	N.A.
7	Triangular	6D	3D	N.A.
8	Triangular	7D	3D	N.A.
9	Triangular	3D	4D	N.A.
10	Triangular	4D	4D	N.A.
11	Triangular	5D	4D	N.A.
12	Triangular	6D	4D	N.A.
13	Triangular	7D	4D	N.A.
14	Triangular	3D	5D	N.A.
15	Triangular	4D	5D	N.A.
16	Triangular	5D	5D	N.A.
17	Triangular	6D	5D	N.A.
18	Triangular	7D	5D	N.A.
19	Staggered	3D	3D	3D
20	Staggered	3D	3D	4D
21	Staggered	3D	3D	5D
22	Staggered	3D	3D	6D
23	Staggered	3D	3D	7D
24	Staggered	3D	3D	8D
25	Staggered	3D	3D	9D
26	Staggered	3D	3D	10D

## RESULTS AND DISCUSSION

As mentioned, the wind turbine performances were assessed through the magnitude of power production. Apart from that, the assessment was done for the wind speed range of 2m/s to 6m/s as stated in literature using Qblade simulation. Unlike previous optimization studies that assume steady mid-latitude wind conditions, this analysis incorporates Malaysia's low wind speed envelope to redefine optimal chord-to-diameter and spacing ratios under tropical offshore constraints.

In Fig. 5, it shows the value of power produced for each of the wind blade diameters in different wind speed conditions. The optimum one will be selected for those that perform better across a range of wind speeds from 2 m/s to 6 m/s. This is important since the wind encountered in Malaysia is low compared to others, therefore wind turbine blade properties with better performance in the variation of low wind speed will be optimum for the final design selection.

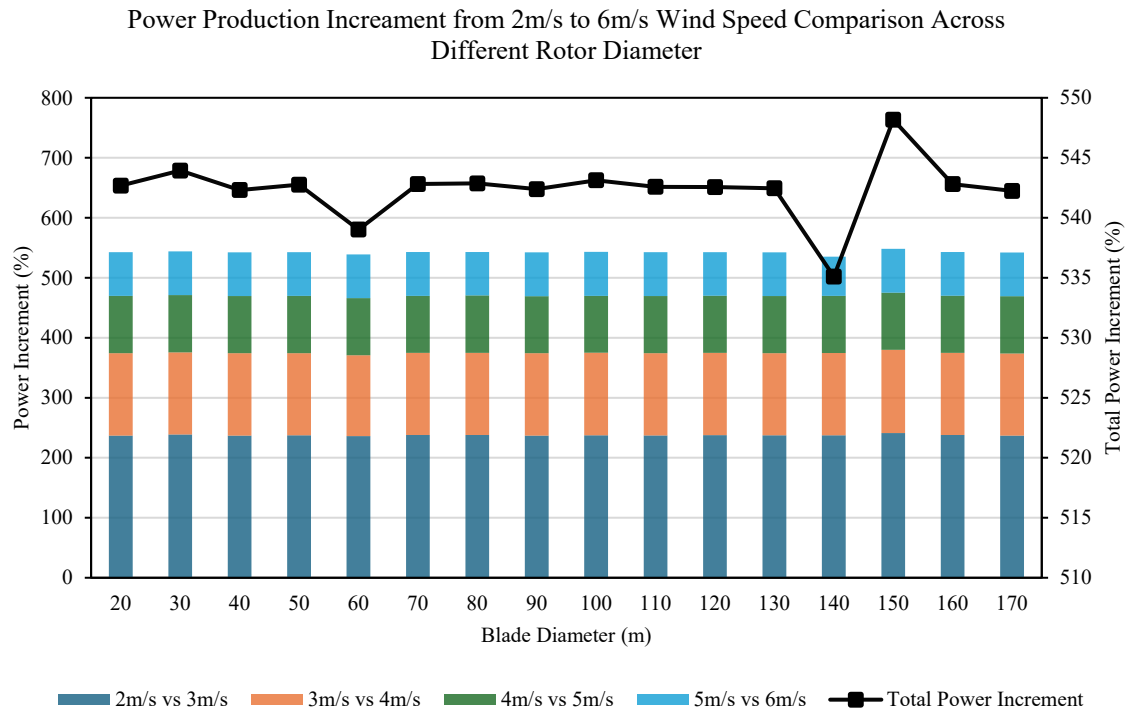


**Figure 5:** Power Production Increment from 2m/s to 6m/s Wind Speed Comparison Across Different Rotor Diameter

Besides, Fig. 5 also shows the power production by each of the wind turbine blade diameters under different wind speed conditions which is ranging from 2m/s to 6m/s. By looking at the percentage of increment of the power production, we can observe that the wind turbine is functioning at its optimum condition with a blade diameter of 150m shown in Fig. 5. Moreover, it has a better increment of power production and a higher power coefficient of the wind turbine,  $C_p = 0.5$ . With higher power coefficient value, the wind turbine can convert more wind energy into electricity.

The blade angle of attack of the wind turbine blade is crucial as well for maximum production. It determines how much is the blade angle facing the wind flow. With an excellent adjustment of blade angle of attack, the ratio of lift to drag can push to the highest value for better performance of the wind turbine.

In Fig. 6, it shows the value of power produced by the 150m diameter wind turbine with the optimization of blade with different blade angle of attack from 0deg to 10deg. The highest power production happened during blade angle of 5deg to 6deg with a glide ratio of approximately 133 shown in Fig. 6 and Fig. 7. This result is further validated by the research by Yass et al. [5] saying NACA 4412 gives better performance in the lift to drag zone of 133.8 and

6deg of angle of attack even with different length of rotor blade.

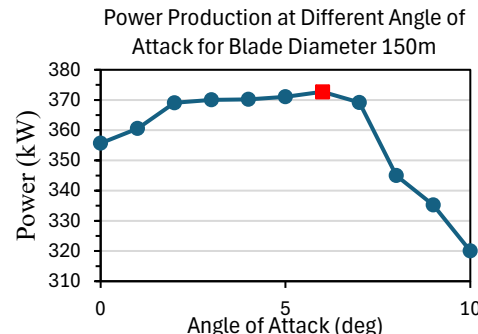


**Figure 6:** Power Production at Different Angle of Attack for Blade Diameter 150m.

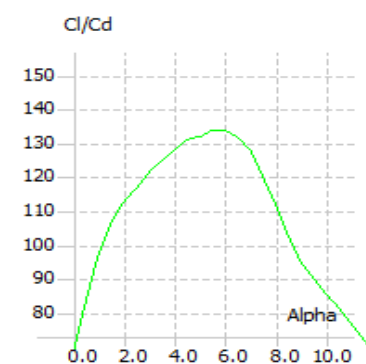


**Figure 7:** Lift to Drag Ratio vs Blade Angle of Attack.

The total power generation of the 3 wind turbines from case 1 to case 3 was calculated and presented, as well as the average power generated by each wind turbine in those 3 cases. The power output of the wind turbines in a 3-turbines side-by-side layout has a similar trend throughout the cases. As illustrated in Figure 8, the central wind turbine produces the greatest amount of power in comparison to the two adjacent wind turbines. It can be inferred that an increase in the separation distance between the wind turbines correlates with enhanced power generation within the wind farm, attributed to the diminishing wake effect.

The 3-turbines triangle arrangement is one group of the Staggered wind farm layout. It was analyzed to obtain the optimal parallel and perpendicular separation distance between the wind turbines. The most optimum distances were applied in the complete Staggered layout analysis. As shown in Fig. 9, a similar trend can also be obtained throughout the cases where 3 wind turbines are arranged in a triangle shape. The middle downstream wind turbine is generating the lowest power as expected compared to the 2 upstream wind turbines. The velocity deficits caused by an upstream wind turbine extracting kinetic energy from the wind lead to decreased power output for downstream wind turbines.

However, the most optimal separation distances between the wind turbines must be determined based on the wind farm's power generated per area. The power production per area ( $m^2$ ) of the wind farm in case 4 is the highest among the cases evaluated for the 3-turbines triangle arrangement. Therefore, the parallel distance of 3D and perpendicular distance of 3D between the upstream and downstream wind turbines are the most optimal configurations, and the separation distances will be applied in the full Staggered layout analysis.

The performance of a full staggered layout for the wind farm was assessed by evaluating the total and average power produced by each turbine. Six

turbines were analyzed from case 19 to case 26, maintaining a constant separation distance of 3d both parallel and perpendicular between turbines, while the distance between two groups of turbines varied from 3D to 10d. The average power output from these turbines is typically lower than that of a triangular layout with three turbines, as illustrated in Fig. 10. This difference may be attributed to the increased wake effect on turbines as the number of turbines in a wind farm rises. Nonetheless, the optimal spacing in a staggered wind farm should be defined by the percentage power difference among the corresponding turbines.

Furthermore, the power generation of the corresponding wind turbines in case 25 has the slightest power difference with only 15.17%. Therefore, it can be concluded that the power generated between both groups of wind turbines is almost the same in case 25. Hence, 9D is the most optimal group distance between the wind turbines in a Staggered wind farm layout.

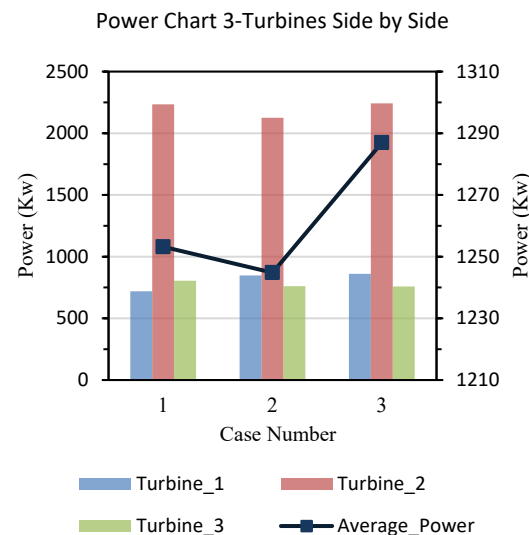


Figure 8: Power Chart for 3-Turbines Side by Side.

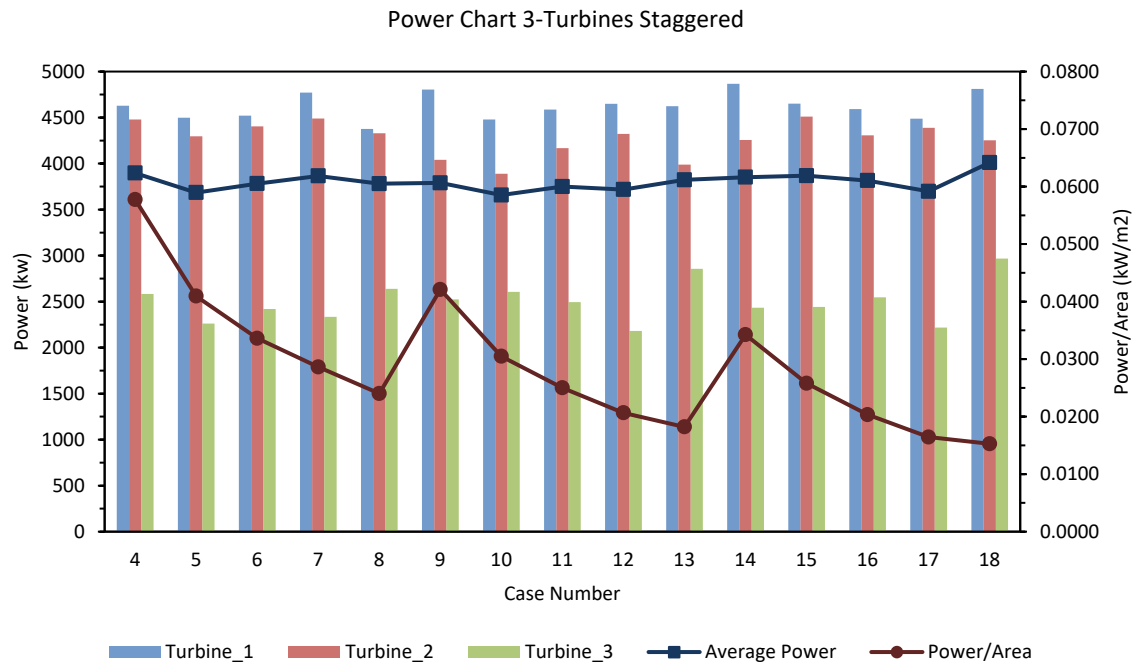


Figure 9: Power Chart for 3-Turbines Staggered.

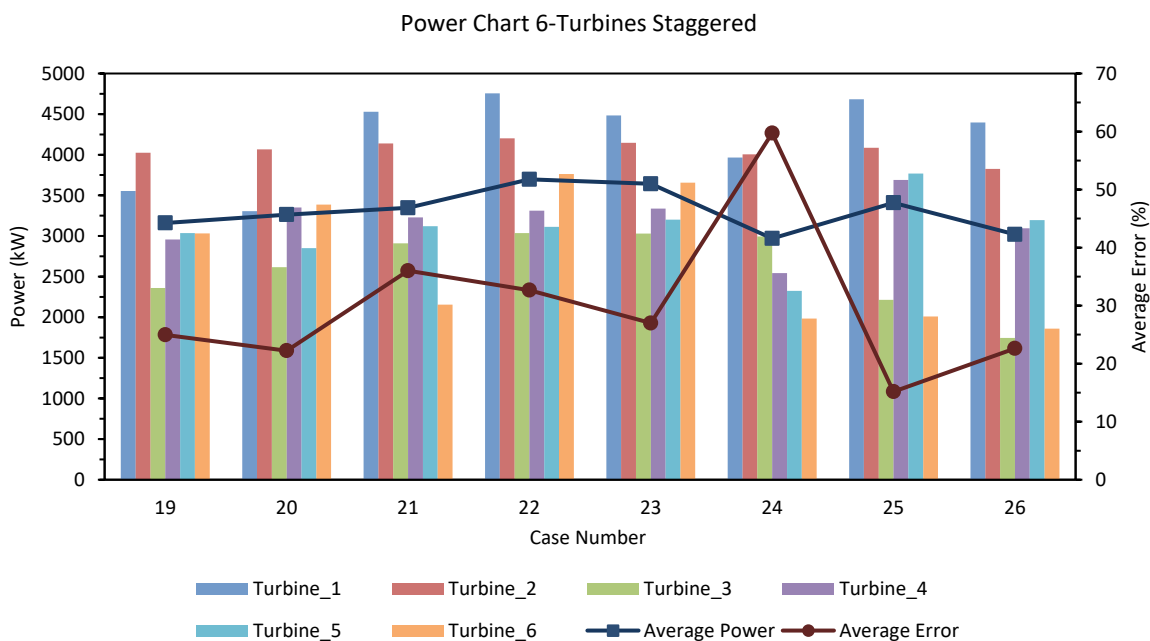


Figure 10: Power Chart for 6-Turbines Staggered.

## CONCLUSION

Despite having a lower annual wind speed, Malaysia satisfies the minimum requirement of 4 m/s necessary for wind energy electricity generation. To optimise wind energy capture in offshore locations, it is vital to improve blade

parameters and choose an appropriate wind farm layout to enhance power generation efficiency. This study identifies an optimal Horizontal Axis Wind Turbine (HAWT) design featuring a blade diameter of 150 meters and an angle of attack of 6 degrees. The optimized blade achieves a higher power coefficient of 0.5. The suggested staggered

wind farm layout comprises specific parallel, perpendicular, and group distances of 3D, 3D, and 9D, respectively, where D represents the turbine diameter. This configuration aims to produce approximately 20,450.83 kW from 6 turbines. Additionally, the proposed layout is expected to generate 0.0577 kW of power per square meter ( $m^2$ ), with a power difference of 15.17% between upstream and downstream turbines. Future studies can expand this framework to other tropical archipelagic zones, using updated 3D wake models and techno-economic validation for Southeast Asian offshore deployment.

## ACKNOWLEDGEMENT

The authors would like to express their gratitude for the financial support from the Ministry of Higher Education Malaysia under the Fundamental Research Grant Scheme (FRGS) (FRGS/1/2020/TK0/UTM/03/4).

## REFERENCES

[1] Lee, J., & Zhao, F. (2021). *Global Wind Report 2021*. [Online]. Available: <http://www.gwec.net/global-figures/wind-energy-global-status/>

[2] Albani, A., Ibrahim, M., & Yong, K. (2014). The feasibility study of offshore wind energy potential in Kijal, Malaysia: A new alternative energy source exploration in Malaysia. *Energy Exploration & Exploitation*, 32(2), 329–344. <https://doi.org/10.1260/0144-5987.32.2.329>.

[3] Hashim, F. E., Peyre, O., Lapok, S. J., Yaakob, O., & Din, A. H. M. (2020). Offshore wind energy resource assessment in Malaysia with satellite altimetry. *Journal of Sustainable Science and Management*, 15(6), 111–124. <https://doi.org/10.46754/jssm.2020.08.010>.

[4] Premono, B. S., Tjahjana, D. D. D. P., & Hadi, S. (2018). Wind energy potential assessment to estimate performance of selected wind turbine in northern coastal region of Semarang, Indonesia. *AIP Conference Proceedings*, 1788, 080009. <https://doi.org/10.1063/1.4968279>.

[5] Yass, M. A. R., Kurdi, S. T., & Shkara, M. A. (2018). Integration of optimum power for wind turbine blade at different cross sections. *Journal of University of Babylon for Engineering Sciences*, 26(7), 1–10.

[6] Patel, J., Savsani, V., Patel, V., & Patel, R. (2019). Layout optimization of a wind farm using a geometric pattern-based approach. *Energy Procedia*, 158, 940–946. <https://doi.org/10.1016/j.egypro.2019.01.233>.

[7] Letcher, T. M. (2017). *Wind Energy Engineering: A Handbook for Onshore and Offshore Wind Turbines*. Elsevier.

[8] Shin, J., Baek, S., & Rhee, Y. (2021). On the development of a metamodel and design-support Excel automation program for offshore wind farm layout optimization. *Journal of Marine Science and Engineering*, 9(2), 148. <https://doi.org/10.3390/jmse9020148>.

[9] Hong, Z., Tao, Y., Guanyu, C., Xiangrui, L., & Yu, H. (2019). Simulation analysis on the blade airfoil of a small wind turbine. *IOP Conference Series: Earth and Environmental Science*, 295(2), 012079. <https://doi.org/10.1088/1755-1315/295/2/012079>.

[10] Choi, N. J., Nam, S. H., Jeong, J. H., & Kim, K. C. (2013). Numerical study on horizontal-axis turbine arrangement in a wind farm: Effect of separation distance on aerodynamic power output. *Journal of Wind Engineering and Industrial Aerodynamics*, 117, 11–17. <https://doi.org/10.1016/j.jweia.2013.04.005>.

[11] Wu, C., Yang, X., & Zhu, Y. (2021). On the design of potential turbine positions for physics-informed optimization of wind farm layout. *Renewable Energy*, 164, 1108–1120. <https://doi.org/10.1016/j.renene.2020.10.060>.